Strengthened Magnetoresistive Epoxy Nanocomposite Papers Derived from Synergistic Nanomagnetite-Carbon Nanofiber Nanohybrids

Hongbo Gu, Jiang Guo, Huige Wei, Shimei Guo, Jiurong Liu,* Yudong Huang, Mojammel Alam Khan, Xuefeng Wang, David P. Young, Suying Wei,* and Zhanhu Guo**

Magnetoresistance (MR), which describes a resistance change upon applying an external magnetic field, is defined as MR = $[R(H) - R(0)]/R(0)$, where $R(0)$ is the resistance without a magnetic field and $R(H)$ is the resistance under a magnetic field of H.[1] Over the past few decades, interest in the MR effect has grown rapidly due to its many applications in magnetic recording systems,[2] especially computer memory and storage systems.[3] To date, the magnetic memory of computers has improved by more than five orders of magnitude in density due to advances in the observed MR effect.[4] Meanwhile, MR-based sensor systems have become a promising platform for biosensing and biochip applications.[5] In addition, a new technology called "spintronics"[6] has emerged over the last few years. Spintronics is a condensed-matter physics field in which the properties of electron spins are studied in order to improve the efficiency of electronic devices and enrich them with new functionalities.[7] Since the Nobel Prize in Physics was awarded to Drs. Fert and Grünberg in 2007 for their discovery of the giant magnetoresistance (GMR) phenomenon,[2b,8] much more attention has been dedicated to this field in order to seek new materials and technologies that meet the requirements for use in the industry. GMR has been reported in carbon nanotubes (CNTs),[9] graphene,[10] conductive polymers,[11] and their nanocomposites.[12] Epoxy resin, as the most commonly used thermosetting resin, has a wide range of applications, including coatings, adhesions, electronics, and aerospace,[13] due to its high tensile strength, low shrinkage during the curing process, and good chemical and corrosion resistance.[14] Although the introduction of magnetic field sensing MR will definitely facilitate the easy detection of structural damage to devices such as marine and aerospace vehicles without any damage to the inherant structure, the occurence of the MR phenomenon in insulating thermosetting systems, and especially in nanocomposites has been rarely reported to date.

Polymer nanocomposites (PNCs) with synergies between the polymer matrix and nanofillers[13,15] show unique mechanical, electrical and thermal properties[14] and have a wide range of applications including biomedical, magneto-optical sensors, data storage devices, and electronic devices.[16,17] However, nanofillers normally have extremely large specific surface areas and intrinsically tend to agglomerate.[18] This agglomeration will cause poor nanofiller compatibility with the polymer matrix and limit the load being transferred from the weak matrix to strong nanofillers, leading to a decrease in mechanical properties.[19] Therefore, obtaining a homogenous dispersion of nanofillers within the polymer matrix is the main challenge for obtaining high quality PNCs.[20] Although functionalization is the commonly used method to improve nanofiller dispersion quality within the polymer matrix and to enhance its mechanical properties,[21] it may lead to a decrease in other properties. For example, COOH-functionalized multi-walled carbon nanotubes (MWNTs) exhibit improved compatibility due to the formation of strong covalent bonds with epoxide groups. Conversely, this approach significantly decreases electrical conductivity becasue of hindered electron transport pathways.[22] Two different nanofiller approaches have been reported for introducing nanoreinforcements.[23] The introduction of a second nanofiller not only increases the nanofiller dispersion quality, but it also provides additional functions to the nanocomposites.[24] For

Dr. H. Gu, Prof. X. Wang
Shanghai Key Lab of Chemical Assessment and Sustainability
Department of Chemistry
Tongji University
Shanghai 200092, China
E-mail: hongbogu2014@tongji.edu.cn

J. Guo, Prof. Z. Guo
Integrated Composites Lab (ICL)
Department of Chemical & Biomolecular Engineering
University of Tennessee
Knoxville, TN 37966, USA
E-mail: zguo10@utk.edu

S. Guo, Prof. J. Liu
Key Laboratory for Liquid–Solid Structural Evolution and Processing of Materials
Ministry of Education and School of Materials Science and Engineering
Shandong University
Jinan, Shandong 250061, China
E-mail: jrliu@sdu.edu.cn

Prof. Y. Huang
School of Chemical Engineering and Technology
Harbin Institute of Technology
Harbin 150001, Heilongjiang, China

M. A. Khan, Prof. D. P. Young
Department of Physics and Astronomy
Louisiana State University
Baton Rouge, LA 70803, USA

H. Wei, Prof. S. Wei
Department of Chemistry and Biochemistry
and Dan F. Smith Department of Chemical Engineering
Lamar University
Beaumont, TX 77710, USA
E-mail: swei@lamar.edu

DOI: 10.1002/adma.201501728

example, Kashiwagi et al.[25] reported reduced flammability in poly(methyl methacrylate) (PMMA) nanocomposites by using a combination of CNTs or carbon nanofibers (CNFs) and nanoclay. Liu et al.[26] reported an increase in electrical conductivity by four orders of magnitude from 10^{-9} to 10^{-5} S cm^{-1} in epoxy nanocomposites with only 0.05 wt% MWNTs by adding an extra 0.2 wt% clay. Shin et al.[27] obtained significantly increased toughness in solution-spun polymer fibers with the combination of CNTs and reduced graphite oxide flakes.

With Fe cations occupying the interstitial tetrahedral and octahedral sites,[28] face centered cubic (fcc) spinel structural magnetite (Fe_3O_4)[29] exhibits excellent magnetic properties for various applications, including telecommunications, data storage, medical diagnosis, drug delivery, and as adsorbents for toxic chemicals.[30] Although CNTs are the most investigated materials among all carbon nanomaterials, becasue of their unique physical properties[15a] including outstanding mechanical and electrical properties,[31] CNFs, with their relatively lower manufacturing costs and good mechanical and electrical properties, are promising candidates for the development of novel structural materials.[32] CNTs are concentric and contain an entirely hollow core, while CNFs are stacked, truncated, conical or planar graphene layers along the filament length.[33] In the last decade, multifunctional papers with conductive, photoluminescent, or magnetic properties have been reported by adding proper fillers into the matrix, which can respond to an external electric field, light, or magnetic field.[34] These papers show great potential for use in energy and environmental applications,[35] as well as in packaging, such as anti-static and electromagnetic interference (EMI) shielding, electronics, and electrochemical materials.[36] Here, novel papers with combined conductive, magnetic and magnetoresistive properties are reported for the first time, derived from epoxy nanocomposites strengthened with 10.0 wt% loading of Fe_3O_4 and 2.0 or 2.5 wt% loading of CNF nanohybrids by a physical mixing process without any surface modification of the nanofiller. The synergistic effect between Fe_3O_4 and CNFs on the properties of the epoxy matrix is studied. The papers derived from epoxy/(2.0 wt%)CNFs and epoxy/(10.0 wt%)Fe_3O_4 nanohybrids have also been fabricated for comparison.

The representative stress–strain curves of these samples are shown in **Figure 1**, and the corresponding tensile properties are summarized in Table S1 of the Supporting Information. The averaged tensile strength (the maximum tensile stress in the stress–strain curve) for the papers coated with pure epoxy (43.16 MPa), epoxy/(10.0 wt%)Fe_3O_4 (31.28 MPa), epoxy/(2.0 wt%)CNFs (45.97 MPa), epoxy/(10.0 wt%)Fe_3O_4/(2.0 wt%)CNFs (47.12 MPa), and epoxy/(10.0 wt%)Fe_3O_4/(2.5 wt%)CNFs (54.48 MPa) samples is remarkably improved by 64.86, 19.48, 75.59, 79.98, and 108.10%, respectively, compared with that of regular paper (26.18 MPa). The averaged Young's modulus (the slope of the stress–strain curve in the low strain range) of regular paper (3.67 GPa) is lower than that of pure epoxy (4.81 GPa), but higher than that of the paper coated with epoxy/(10.0 wt%)Fe_3O_4 (2.85 GPa), epoxy/(2.0 wt%)CNFs (2.50 GPa), epoxy/(10.0 wt%)Fe_3O_4/(2.0 wt%)CNFs (2.68 GPa), and epoxy/(10.0 wt%)Fe_3O_4/(2.5 wt%)CNFs (2.12 GPa). Generally, the Young's modulus is used to represent the elastic behavior of a material.[37] The increased Young's modulus in epoxy

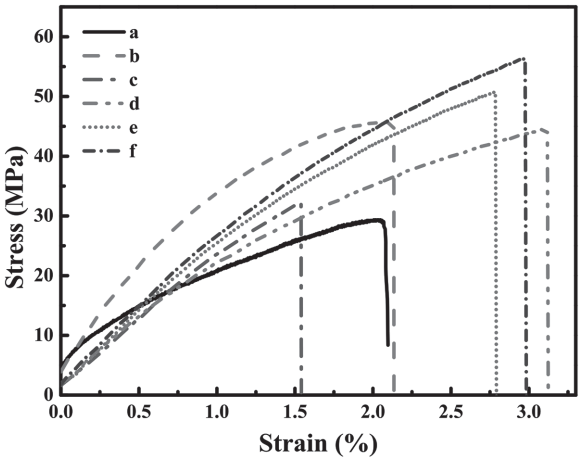

Figure 1. Stress–strain curves of a) regular paper, b) paper coated with pure epoxy, c) epoxy/(10.0 wt%)Fe_3O_4, d) epoxy/(2.0 wt%)CNFs, e) epoxy/(10.0 wt%)Fe_3O_4/(2.0 wt%)CNFs, and f) epoxy/(10.0 wt%)Fe_3O_4/(2.5 wt%)CNFs.

paper composite samples arises from the stiff interfacial layer formed between the epoxy and the paper, which makes deformation of the paper difficult to achieve.[15a] The elongation-at-break of regular paper (1.93%) is higher than that of the paper coated with pure epoxy (1.46%) and epoxy/(10.0 wt%)Fe_3O_4 (1.73%), but lower than that of the papers coated with epoxy/(2.0 wt%)CNFs, epoxy/(10.0 wt%)Fe_3O_4/(2.0 wt%)CNFs and epoxy/(10.0 wt%)Fe_3O_4/(2.5 wt%)CNFs (2.10, 2.53, and 3.02%, respectively). The modulus of toughness (U_t), i.e. the energy required to completely fracture the materials, is correlated to the fracture toughness and described as the area under the stress–strain curve.[38] The U_t for regular paper, paper coated with epoxy, epoxy/(10.0 wt%)Fe_3O_4, epoxy/(2.0 wt%)CNFs, epoxy/(10.0 wt%)Fe_3O_4/(2.0 wt%)CNFs, and epoxy/(10.0 wt%)Fe_3O_4/(2.5 wt%)CNFs were calculated to be 42.35, 27.96, 67.84, 86.93, 84.85, and 100.72 MJ m^{-3} (or MPa), respectively. The U_t of the paper coated with pure epoxy, epoxy/(2.0 wt%)CNFs, epoxy/(10.0 wt%)Fe_3O_4/(2.0 wt%)CNFs, and epoxy/(10.0 wt%)Fe_3O_4/(2.5 wt%)CNFs is increased by 60.19, 105.27, 100.38, and 137.83%, respectively, compared with that of regular paper. The improved mechanical properties indicate that the introduced second phase Fe_3O_4 nanoparticles can significantly increase the tensile strength of the papers coated with epoxy/CNFs PNCs. Normally, the two nanofiller strategy and the synergistic interactions between two nanofillers can efficiently increase their dispersion quality in the matrix. This has been observed in poly(phenylene sulfide) nanocomposites with SWNTs and tungsten disulfide (WS_2) nanoparticles,[39] in which fullerene-like WS_2 nanoparticles behaved as a solid lubricant to provide the materials with anti-friction and anti-wear properties. Here, pure CNFs without any modification show weak adhesion with the epoxy matrix and are easy to agglomerate, **Scheme 1**a, leading to poor dispersion of the CNFs within the epoxy matrix and a lower tensile strength (Table S1 of the Supporting Information). However, after adding the spherical Fe_3O_4 nanoparticles, the synergistic interactions between CNFs and Fe_3O_4 can restrict the entanglement of each nanofiller and make them less agglomerated, Scheme 1b, leading to a better

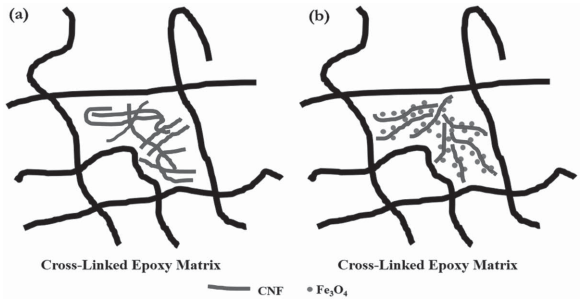

Scheme 1. Proposed dispersion mechanism: a) agglomerated CNFs and b) after mixing with Fe_3O_4 nanoparticles in the cross-linked epoxy matrix.

dispersion quality and enhanced tensile strength as shown in Table S1 of the Supporting Information.

Figure 2 shows SEM microstructures of the fracture surface after tensile tests. At the micrometer scale, rough fracture surfaces are observed for papers coated with epoxy/(2.0 wt%)CNFs and epoxy/(10.0 wt%)Fe_3O_4/(2.5 wt%)CNFs, Figure 2a,c. In the enlarged image of the fracture surface of epoxy/(2.0 wt%)CNFs, Figure 2b, the CNFs are observed to be connected to each other, and the formed network is beneficial for electron transport within the CNFs. In the epoxy/(10.0 wt%)Fe_3O_4/(2.5 wt%) CNFs, Figure 2c,d, the CNFs could be pulled out with the epoxy adhered to the CNFs, indicating an excellent interfacial interaction between the polymer matrix and the reinforced CNFs.[15a] The Fe_3O_4 nanoparticles are uniformly distributed within the epoxy matrix without agglomeration, Figure S2a,b of the Supporting Information, further confirming the proposed nanofiller dispersion mechanism, Scheme 1b.

The resistivity of the paper coated with epoxy/(2.0 wt%) CNFs, **Figure 3**A(a), changes from 1.45×10^4 Ω cm at 50 K to 1.21×10^4 Ω cm at 290 K. The temperature-dependent resistivity of the paper coated with epoxy/(10.0 wt%)Fe_3O_4 PNCs cannot be measured since its resistivity is beyond the range of the equipment (the resistivity limit is $<10^6$ Ω cm). Compared

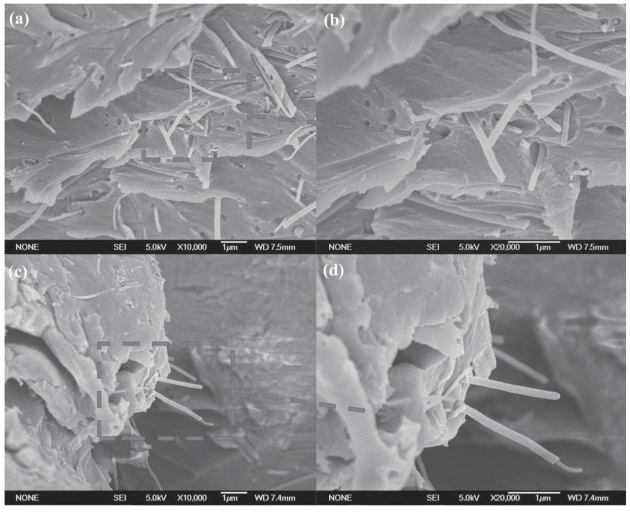

Figure 2. SEM images of the fracture surface for a) epoxy/(2.0 wt%) CNFs, and c) epoxy/(10.0 wt%)Fe_3O_4/(2.5 wt%)CNFs samples. The correspoding enlarged images are shown in panels (b) and (d), respectively.

to the paper coated with epoxy/(2.0 wt%)CNFs, a decreased resistivity from 4.2×10^3 Ω cm at 50 K to 3.6×10^3 Ω cm at 290 K, Figure 3A(b), was observed in the epoxy/(10.0 wt%) Fe_3O_4/(2.0 wt%)CNFs. The resistivity of the paper coated with epoxy/(10.0 wt%)Fe_3O_4/(2.5 wt%)CNFs sample changed from 244.15 Ω cm at 50 K to 226.23 Ω cm at 290 K, lower than that of the paper coated with epoxy/(10.0 wt%)Fe_3O_4/(2.0 wt%) CNFs, as shown in Figure 3A(c). The synergistic interaction between the two nanofillers, Fe_3O_4 and CNFs, can prevent the agglomoration of the nanofillers, Scheme 1b, and help the formation of continuous conductive networks within the epoxy matrix, causing the decreased resistivity in the papers coated with epoxy/Fe_3O_4/CNF nanohybrids compared to the papers coated with epoxy/CNF as mentioned above. In Figure 3A(a,c), the resistivity of the papers coated with epoxy/(2.0 wt%)CNFs and epoxy/(10.0 wt%)Fe_3O_4/(2.5 wt%)CNFs decreases with increasing temperature until 230 K, indicating a semiconductive behavior[29] with a negative temperature coefficient,[40] and thereafter is slightly increased with increasing temperature. In Figure 3A(b), the resistivity of the paper coated with epoxy/(10.0 wt%)Fe_3O_4/(2.0 wt%)CNFs shows a unique temperature-dependent behavior, which decreases with increasing temperature below 195 K, indicating semiconducting behavior with a negative temperature coefficient, but then increases when the temperature is further increased, exhibiting a positive temperature coefficient.[41] Normally, a positive temperature coefficient of resistivity indicates metallic conduction, whereas a negative temperature coefficient of resistance represents thermally activated behavior,[42] in which the conductivity is controlled by tunneling or the hopping of charges between nanofillers through the interlayer of a non-conducting epoxy polymer matrix.[43]

Normally, MR is observed in molecules with π-conjugated chemical structures and a relatively small energy gap ranging from about 1.5 to 3.5 eV, such as rubrene and Alq_3,[44] in which the P_z orbitals of the electrons can overlap with the P_z orbitals of the neighboring carbons along the chains to form a delocalized π-bond after sp^2 hybridization. CNFs, which are formed by a sp^2-based linear filament with a diameter of about 100 nm, similar to CNTs[45] and graphene,[46] have potential applications in MR (the chemical structure of the CNFs is shown in Figure S3 of the Supporting Information). Fe_3O_4 is a half-metallic material with the coexistence of a metallic nature for one electron spin and an insulating nature for the other, in which the density of states at the Fermi level ($N(E_F)$) is completely polarized, and the electrons can hop between Fe^{2+} and Fe^{3+} ions in the octahedral sites at room temperature.[15b] An increased MR of up to 42% was reported after adding 30.0 wt% Fe_3O_4 nanoparticles to the polyaniline (PANI) matrix compared to that observed in pure PANI (53%),[29] illustrating that the addition of Fe_3O_4 has a significant effect on the MR properties of the polymer matrix.[47]

Figure 3B shows the measured MR of the prepared epoxy paper nanohybrids. Negative MR values of –0.75, –0.96, and –0.33% are observed for the papers coated with epoxy/(2.0 wt%) CNFs, epoxy/(10.0 wt%)Fe_3O_4/(2.0 wt%)CNFs, and epoxy/(10.0 wt%)Fe_3O_4/(2.5 wt%)CNFs in a magnetic field of 9 T (= 90 000 Oe) at room temperature, in which the magnetic field was applied perpendicular to the sample, Figure 3B(a–c). To our knowledge, no MR effect has been reported in epoxy and its

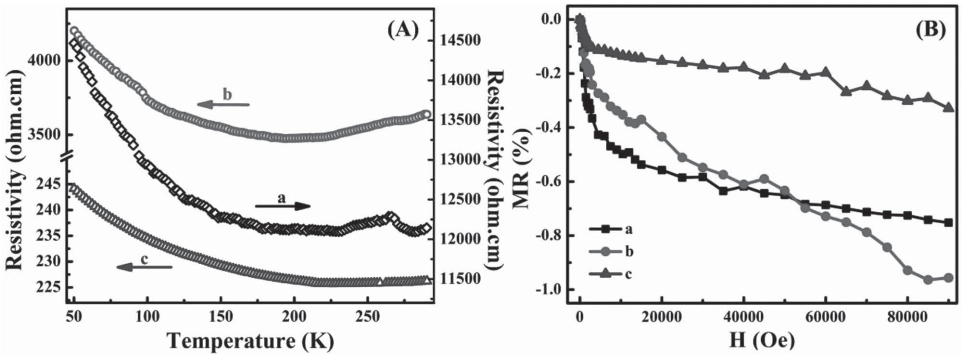

Figure 3. A) Resistivity versus temperature curves of a) epoxy/(2.0 wt%)CNFs, b) epoxy/(10.0 wt%)Fe_3O_4/(2.0 wt%)CNFs, and c) epoxy/(10.0 wt%)Fe_3O_4/(2.5 wt%)CNFs. B) Room temperature magnetoresistance of a) epoxy/(2.0 wt%)CNFs, b) epoxy/(10.0 wt%)Fe_3O_4/(2.0 wt%)CNFs, and c) epoxy/(10.0 wt%)Fe_3O_4/(2.5 wt%)CNFs.

nanocomposites so far. Although these MR values are not large, they are still slightly higher than that in the $La_{0.7}Sr_{0.3}MnO_3$ (LSMO)/poly(3-hexylthiophene-2,5-diyl) (rr-P3HT) system (0.3%).[48] Interestingly, the MR value observed in these epoxy nanohybrids is negative within the measured magnetic field range and increases with increasing the magnetic field. This indicates that a magnetic field is beneficial for electrical transport within the epoxy matrix. The spin current has replaced the electrical current in electronics under a magnetic field after the observation of GMR phenonmenon.[49]

The proposed MR mechanism in these nanohybrids is shown in **Scheme 2**. In the epoxy/(2.0 wt%)CNFs paper sample, the CNFs exhibit paramagnetic properties after applying a magnetic field, in which the electron spins are aligned with the external magnetic field,[50] leading to increased electrical conductivity. In principle, materials with unpaired electrons (or spins) can be paramagnetic. Each electron has a magnetic moment and spin angular momentum of $S = 1/2$ with the spin quantum number $m_s = +1/2$ and $m_s = -1/2$.[1] Under an external magnetic field H, the magnetic moment of the electron spins is aligned either parallel ($m_s = +1/2$) or antiparallel ($m_s = -1/2$) to the magnetic field. The improved energy state of electron spins due to the Zeeman effect (which is a spin-splitting effect under the applied magnetic field[51]) can be expressed with the following equation: $E = m_s g_e \mu_B H$,[52] where m_s is the spin quantum number, g_e is the Zeeman g-factor, and μ_B is the Bohr magneton. In the absence of a magnetic field, the two quantum states with spin quantum numbers $m_s = +1/2$ and $m_s = -1/2$ have the same energy level, which is called spin degeneracy. In the presence of a magnetic field, the separation between the upper and lower energy states is $\Delta E = h\nu = g_e \mu_B H$ for the unpaired free electrons occurred, where $h\nu$ is the phonon energy corresponding to a specific frequency. The electron spins in the paramagnetic CNFs are aligned after applying a magnetic field to the synthesized epoxy/(2.0 wt%)CNFs paper sample, leading to the increased electrical transport efficiency and negative MR, Scheme 2a.

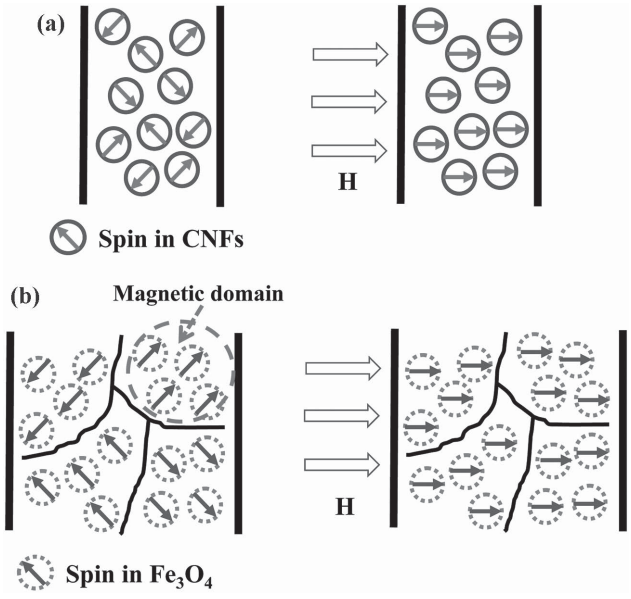

Scheme 2. Proposed mechanism for the observed MR in a) epoxy/(2.0 wt%)CNFs; and b) epoxy/(10.0 wt%)Fe_3O_4/(2.0 wt%)CNFs samples.

Owing to its half-metallic nature with high spin polarization, Fe_3O_4 is a promising material for serving as spin injection electrodes.[53] Generally, ferromagnetic materials consist of different magnetic domains that are groups of atomic magnets formed by their interaction or exchange coupling. The magnetic moment of atoms is aligned in the same direction in one individual magnetic domain, but at different directions in different domains.[54] However, the magnetic moment of atoms in different domains will tend to be aligned in the same direction after applying a magnetic field and this alignment depends on the magnetic field strength, which is called the magnetization process.[54] This magnetization will increase with an increasing magnetic field until the saturation magnetization is reached. In the epoxy/(10.0 wt%)Fe_3O_4/(2.0 wt%)CNFs sample, the high spin-polarized and ferromagnetic Fe_3O_4 nanoparticles can align the metallic spin-magnetic moment along the applied magnetic field to form a spin-polarized current, which increases with increased magnetic field strength. The increased spin-polarized current with increasing magnetic field leads to a decreased resistivity and higher negative MR values (–0.96% at 9 T) in the papers coated with epoxy/(10.0 wt%)Fe_3O_4/(2.0 wt%)CNFs nanohybrids compared with that of the papers coated with epoxy/(2.0 wt%)CNF nanohybrids (–0.75% at 9 T), Scheme 2b. In the papers coated with epoxy/(10.0 wt%)Fe_3O_4/(2.5 wt%)CNFs

sample, the negative MR value of –0.33% at 9 T is lower than that in the papers coated with epoxy/(10.0 wt%)Fe_3O_4/(2.0 wt%)CNFs. The increased amount of CNFs in the epoxy may hinder the distribution of magnetic domains of Fe_3O_4 nanoparticles, which is not beneficial for the alignment of the magnetic moment and the formation of a spin-polarized current. Therefore, the electrical transport paths in the papers coated with epoxy/(10.0 wt%)Fe_3O_4/(2.5 wt%)CNFs are hampered, resulting in a decreased negative MR signal. Normally, the slope at a low magnetic field (around 0.2 T) can reflect the sensitivity of a material to the applied magnetic field.[42] The slope of the papers coated with epoxy/(2.0 wt%)CNFs, epoxy/(10.0 wt%)Fe_3O_4/(2.0 wt%)CNFs, and epoxy/(10.0 wt%)Fe_3O_4/(2.5 wt%)CNFs follows the relationship: epoxy/(2.0 wt%)CNFs > epoxy/(10.0 wt%)Fe_3O_4/(2.0 wt%)CNFs > epoxy/(10.0 wt%)Fe_3O_4/(2.5 wt%)CNFs. Materials with a high magnetic field sensitivity can serve as magnetic field sensors.[12a]

In summary, conductive magnetic epoxy nanocomposite papers consisting of epoxy/Fe_3O_4/CNFs nanohybrids that show magnetoresistive behavior are reported. An enhanced tensile strength of the prepared epoxy paper nanohybrids is observed compared with that of regular paper due to the synergies between Fe_3O_4 nanoparticles and CNFs. The paramagnetic property of the CNFs is proposed to induce a negative MR effect in the epoxy/CNF nanohybrids, and the spin-polarized current formed by the ferromagnetic Fe_3O_4 nanoparticles is proposed to contribute to the observed negative MR phenomenon in the epoxy/Fe_3O_4/CNF nanohybrids. These multifunctional nanocomposite papers have potential applications for flexible eletronics, magnetoresistive sensors and the printing industry.

Experimental Section

Preparation of Epoxy/Fe_3O_4/CNF Nanohybrid Suspensions: As-received Fe_3O_4 nanoparticles (10.0 wt%, average size of 12 nm, obtained from Nanjing Emperor Nano Material Co., Ltd.) were immersed in Epon 862 resin (bisphenol F epoxy, Miller-Stephenson Chemical Company, Inc., chemical structure shown in Figure S1 of the Supporting Information) overnight without any disturbance so that the resin could wet the nanoparticles and the solution was then sonicated (Branson 5510) for 30 min. The above solution was then poured into a beaker (100 mL) containing CNFs with a loading of 2.0 or 2.5 wt% until the CNFs were wetted by the Fe_3O_4/epoxy suspensions. Next, the epoxy/Fe_3O_4/CNF nanohybrid suspension was mechanically stirred for one hour (600 rpm, Heidolph, RZR 2041). All procedures were carried out at room temperature.

Fabrication of Epoxy/Fe_3O_4/CNF Nanohybrid Papers: The curing agent EpiCure W (Miller-Stephenson Chemical Company, Inc., chemical structure shown in Figure S1 of the Supporting Information) was added into the above prepared epoxy/Fe_3O_4/CNF nanohybrid suspension with a monomer/curing agent weight ratio of 100/26.5 following the recommendation of the Miller-Stephenson Chemical Company, followed by one hour of mechanical stirring (200 rpm). The solution was then mechanically stirred at 85 °C for 0.5 h in a water bath at the same speed (200 rpm), which was essential for removing bubbles and preventing the sedimentation of nanofillers during the curing process. Finally, the solutions were painted onto print paper (Universal Multipurpose Paper, UNV 95200, BettyMills Company) with a spatula, cured at 120 °C for 5 h, and then cooled down to room temperature naturally. These samples were indexed as epoxy/(10.0 wt%)Fe_3O_4/(2.0 wt%)CNFs and epoxy/(10.0 wt%)Fe_3O_4/(2.5 wt%)CNFs, respectively. The papers derived from pure epoxy, epoxy/Fe_3O_4 PNCs filled with 10.0 wt% Fe_3O_4, epoxy/CNFs PNCs containing 2.0 wt% CNFs were also fabricated following the above procedures for comparison and labeled as epoxy/(10.0 wt%)Fe_3O_4 and epoxy/(2.0 wt%)CNFs, respectively. Epoxy/CNFs PNCs filled with 2.5 wt% loading of CNFs were also prepared in this work. However, the viscosity of epoxy/CNFs suspension filled with 2.5 wt% loading of CNFs was too viscous due to the agglomeration of CNFs, which broke down easily during the tensile test. Therefore, the properties of epoxy/CNFs PNCs filled with 2.5 wt% loading of CNFs were not investigated in this work.

Characterization: The magnetic paper was cut into a 3.0 cm × 1.0 cm rectangular shape to perform the temperature dependent resistivity and MR measurements. The resistivity was measured by a standard four-probe method over a temperature range of 50 to 290 K. The MR was carried out using a standard four-probe technique by a 9-Tesla Physical Properties Measurement System (PPMS) by Quantum Design at room temperature. The four probes were 0.002 inch diameter platinum wires, which were attached by silver paste to the sample, and the magnetic field was applied perpendicular to the sample. The nanofiller distribution within the matrix was observed by a field emission scanning electron microscope (FE SEM, JEOL, JSM-6700F system). The samples were prepared by adhering the powders to an aluminum plate. The tensile tests were carried out following the American Society for Testing and Materials (ASTM, 2002, standard D412–98a) in a unidirectional tensile test machine (ADMET universal testing system, eXpert 2610). The parameters (displacement and force) were controlled by a digital controller (MTESTQuattro) with MTESTQuattro Materials Testing Software. Rectangular shaped samples (6.0 cm × 1.0 cm) were prepared for the tests. A crosshead speed of 1 mm min^{-1} was used, and the strain (mm mm^{-1}) was calculated by dividing the jogging displacement by the original gauge length.

Supporting Information

Supporting Information is available from Wiley Online Library or from the author.

Acknowledgments

This work was financially supported by the National Science Foundation (NSF) - Nanomanufacturing under the EAGER program (CMMI 13–14486), Nanoscale Interdisciplinary Research Team and Materials Processing and Manufacturing (CMMI 10–30755) and Chemical and Biological Separations under the EAGER program (CBET 11–37441). The start-up fund from the University of Tennessee is also acknowledged. This work was also supported by the Shanghai Science and Technology Commission (14DZ2261100). H.G. thanks the Science and Technology Commission of Shanghai Municipality (No. 15YF1412700) and Tongji University (No. 2014KJ028) for financial support. J.L. is thankful for financial support from the Doctoral Program of Higher Education of China (20130131110068), and the Natural Science Fund for Distinguished Young Scholars of Shandong (JQ201312). D.P.Y. acknowledges support from the NSF under Grant No. DMR 1306392.

Received: April 12, 2015
Revised: July 20, 2015
Published online: September 2, 2015

[1] H. Gu, X. Zhang, H. Wei, Y. Huang, S. Wei, Z. Guo, *Chem. Soc. Rev.* **2013**, *13*, 5907.
[2] a) Z. Guo, S. Park, H. T. Hahn, S. Wei, M. Moldovan, A. B. Karki, D. P. Young, *Appl. Phys. Lett.* **2007**, *90*, 053111; b) P. A. Grünberg, *Rev. Mod. Phys.* **2008**, *80*, 1531.

[3] W. J. Gallagher, S. S. P. Parkin, *IBM J. Res. Dev.* **2006**, *50*, 5.
[4] a) G. W. Burr, B. N. Kurdi, J. C. Scott, C. H. Lam, K. Gopalakrishnan, R. S. Shenoy, *IBM J. Res. Dev.* **2008**, *52*, 449; b) R. F. Freitas, W. W. Wilcke, *IBM J. Res. Dev.* **2008**, *52*, 439.
[5] a) D. L. Graham, H. A. Ferreira, P. P. Freitas, *Trends Biotechnol.* **2004**, *22*, 455; b) Y. Li, B. Srinivasan, Y. Jing, X. Yao, M. A. Hugger, J.-P. Wang, C. Xing, *J. Am. Chem. Soc.* **2010**, *132*, 4388.
[6] I. Malajovich, J. J. Berry, N. Samarth, D. D. Awschalom, *Nature* **2001**, *411*, 770.
[7] F. Pulizzi, *Nat. Mater.* **2012**, *11*, 367.
[8] A. Fert, *Angew.Chem. Int. Ed.* **2008**, *47*, 5956.
[9] J. Zhu, H. Gu, Z. Luo, N. Haldolaarachige, D. P. Young, S. Wei, Z. Guo, *Langmuir* **2012**, *28*, 10246.
[10] F. Muñoz-Rojas, J. Fernández-Rossier, J. J. Palacios, *Phys. Rev. Lett.* **2009**, *102*, 136810.
[11] H. Gu, J. Guo, X. Yan, H. Wei, X. Zhang, J. Liu, Y. Huang, S. Wei, Z. Guo, *Polymer* **2014**, *55*, 4405.
[12] a) H. Gu, J. Guo, X. Zhang, Q. He, Y. Huang, H. A. Colorado, N. S. Haldolaarachchige, H. L. Xin, D. P. Young, S. Wei, Z. Guo, *J. Phys. Chem. C* **2013**, *117*, 6426; b) H. Gu, J. Guo, Q. He, Y. Jiang, Y. Huang, N. Haldolaarachige, Z. Luo, D. P. Young, S. Wei, Z. Guo, *Nanoscale* **2014**, *6*, 181; c) H. Gu, J. Guo, H. Wei, X. Zhang, J. Zhu, L. Shao, Y. Huang, N. Haldolaarachchige, D. P. Young, S. Wei, Z. Guo, *Polymer* **2014**, *55*, 944.
[13] H. Gu, S. Tadakamalla, Y. Huang, H. A. Colorado, Z. Luo, N. Haldolaarachchige, D. P. Young, S. Wei, Z. Guo, *ACS Appl. Mater. Interfaces* **2012**, *4*, 5613.
[14] Y. Zhao, E. V. Barrera, *Adv. Funct. Mater.* **2010**, *20*, 3039.
[15] a) H. Gu, S. Tadakamalla, X. Zhang, Y.-D. Huang, Y. Jiang, H. A. Colorado, Z. Luo, S. Wei, Z. Guo, *J. Mater. Chem. C* **2013**, *1*, 729; b) J. Guo, H. Gu, H. Wei, Q. Zhang, N. Haldolaarachchige, Y. Li, D. P. Young, S. Wei, Z. Guo, *J. Phys. Chem. C* **2013**, *117*, 10191.
[16] R. T. Olsson, M. A. Samir, G. Salazar-Alvarez, L. Belova, V. Ström, L. A. Berglund, O. Ikkala, J. Nogues, U. W. Gedde, *Nat. Nanotechnol.* **2010**, *5*, 584.
[17] O. Gutfleisch, M. A. Willard, E. Brück, C. H. Chen, S. G. Sankar, J. P. Liu, *Adv. Mater.* **2011**, *23*, 821.
[18] Y. Li, X. Wang, J. Sun, *Chem. Soc. Rev.* **2012**, *41*, 5998.
[19] Z. Guo, X. Liang, T. Pereira, R. Scaffaro, H. Thomas Hahn, *Compos. Sci. Technol.* **2007**, *67*, 2036.
[20] H. Gu, J. Guo, Q. He, S. Tadakamalla, X. Zhang, X. Yan, Y. Huang, H. A. Colorado, S. Wei, Z. Guo, *Ind. Eng. Chem. Res.* **2013**, *52*, 7718.
[21] T. M. Terrones, O. Martín, M. González, J. Pozuelo, B. Serrano, J. C. Cabanelas, S. M. Vega-Díaz, J. Baselga, *Adv. Mater.* **2011**, *23*, 5302.
[22] L. Guadagno, B. De Vivo, A. Di Bartolomeo, P. Lamberti, A. Sorrentino, V. Tucci, L. Vertuccio, V. Vittoria, *Carbon* **2011**, *49*, 1919.
[23] C. Zhang, W. W. Tjiu, T. Liu, W. Y. Lui, I. Y. Phang, W.-D. Zhang, *J. Phys. Chem. B* **2011**, *115*, 3392.
[24] E. Bilotti, H. Zhang, H. Deng, R. Zhang, Q. Fu, T. Peijs, *Compos. Sci. Technol.* **2013**, *74*, 85.
[25] T. Kashiwagi, F. Du, J. F. Douglas, K. I. Winey, R. H. Harris, J. R. Shields, *Nat. Mater.* **2005**, *4*, 928.
[26] L. Liu, J. C. Grunlan, *Adv. Funct. Mater.* **2007**, *17*, 2343.
[27] M. K. Shin, B. Lee, S. H. Kim, J. A. Lee, G. M. Spinks, S. Gambhir, G. G. Wallace, M. E. Kozlov, R. H. Baughman, S. J. Kim, *Nat. Commun.* **2012**, *3*, 650.
[28] S. Sun, H. Zeng, *J. Am. Chem. Soc.* **2002**, *124*, 8204.
[29] H. Gu, Y. Huang, X. Zhang, Q. Wang, J. Zhu, L. Shao, N. Haldolaarachchige, D. P. Young, S. Wei, Z. Guo, *Polymer* **2012**, *53*, 801.
[30] Y. Yu, A. Mendoza-Garcia, B. Ning, S. Sun, *Adv. Mater.* **2013**, *25*, 3090.
[31] a) H. Gu, S. B. Rapole, Y. Huang, D. Cao, Z. Luo, S. Wei, Z. Guo, *J. Mater. Chem. A* **2013**, *1*, 2011; b) X. Wang, Q. Li, J. Xie, Z. Jin, J. Wang, Y. Li, K. Jiang, S. Fan, *Nano Lett.* **2009**, *9*, 3137.
[32] a) J. Zhu, S. Wei, J. Ryu, M. Budhathoki, G. Liang, Z. Guo, *J. Mater. Chem.* **2010**, *20*, 4937; b) J. Zhu, S. Wei, A. Yadav, Z. Guo, *Polymer* **2010**, *51*, 2643.
[33] *Springer Handbook of Nanomaterials*, Springer-Verlag, Berlin Heidelberg, Germany **2013**, p. 243.
[34] O. C. Compton, D. A. Dikin, K. W. Putz, L. C. Brinson, S. T. Nguyen, *Adv. Mater.* **2010**, *22*, 892.
[35] L. Hu, Y. Cui, *Energy Environ. Sci.* **2012**, *5*, 6423.
[36] X. Zhao, C. M. Hayner, M. C. Kung, H. H. Kung, *ACS Nano* **2011**, *5*, 8739.
[37] B. Rubehn, T. Stieglitz, *Biomaterials* **2010**, *31*, 3449.
[38] S. Chatterjee, F. Nüesch, B. T. Chu, *Nanotechnology* **2011**, *22*, 275714.
[39] M. Naffakh, A. M. Diez-Pascual, C. Marco, G. Ellis, *J. Mater. Chem.* **2012**, *22*, 1418.
[40] S. Cho, S. M. Kauzlarich, J. Olamit, K. Liu, F. Grandjean, L. Rebbouh, G. J. Long, *J. Appl. Phys.* **2004**, *95*, 6804.
[41] Q. Wan, Q. Li, Y. Chen, T. Wang, X. He, X. Gao, J. Li, *Appl. Phys. Lett.* **2004**, *84*, 3085.
[42] S.-J. Cho, J.-C. Idrobo, J. Olamit, K. Liu, N. D. Browning, S. M. Kauzlarich, *Chem. Mater.* **2005**, *17*, 3181.
[43] J. Vilčáková, P. Sáha, O. Quadrat, *Eur. Polym. J.* **2002**, *38*, 2343.
[44] Ö. Mermer, G. Veeraraghavan, T. L. Francis, Y. Sheng, D. T. Nguyen, M. Wohlgenannt, A. Köhler, M. K. Al-Suti, M. S. Khan, *Phys. Rev. B* **2005**, *72*, 205202.
[45] M. Urdampilleta, S. Klyatskaya, J. P. Cleuziou, M. Ruben, W. Wernsdorfer, *Nat. Mater.* **2011**, *10*, 502.
[46] J. Bai, R. Cheng, F. Xiu, L. Liao, M. Wang, A. Shailos, K. L. Wang, Y. Huang, X. Duan, *Nat. Nanotechnol.* **2010**, *5*, 655.
[47] A. Ozbay, E. R. Nowak, Z. G. Yu, W. Chu, Y. Shi, S. Krishnamurthy, Z. Tang, N. Newman, *Appl. Phys. Lett.* **2009**, *95*, 232507.
[48] C. Chappert, A. Fert, F. N. Van Dau, *Nat. Mater.* **2007**, *6*, 813.
[49] S. Wang, P. Guo, P. Wu, Z. Han, *Macromolecules* **2004**, *37*, 3815.
[50] A. G. Aronov, S. Hikami, A. I. Larkin, *Phys. Rev. Lett.* **1989**, *62*, 965.
[51] J. Zhu, M. Chen, H. Qu, Z. Luo, S. Wu, H. A. Colorado, S. Wei, Z. Guo, *Energy Environ. Sci.* **2013**, *6*, 194.
[52] D. Zhang, Z. Liu, S. Han, C. Li, B. Lei, M. P. Stewart, J. M. Tour, C. Zhou, *Nano Lett.* **2004**, *4*, 2151.
[53] U. Welp, V. Vlasko-Vlasov, X. Liu, J. Furdyna, T. Wojtowicz, *Phys. Rev. Lett.* **2003**, *90*, 167206.
[54] *Introduction to Magnetic Materials, 2nd Edition*, John Wiley & Sons, Inc., Hoboken, NJ **2009**.